Vibration and flow characteristics near cavitation occurrence in mixed-flow pump

To cite this article: H M Yang *et al* 2019 *IOP Conf. Ser.: Earth Environ. Sci.* **240** 062032

Vibration and flow characteristics near cavitation occurrence in mixed-flow pump

H M Yang[1], K Y Lee[1], J H Kim[1] and Y S Choi[1]

[1]Thermal & Fluid Systems Group, Korea Institute of Industrial Technology, 89 Yangdaegiro-gil, Ipjang-myeon, Seobuk-gu, Cheonan-si, 31056, Republic of Korea

E-mail: yhm0430@kitech.re.kr, chrisst@kitech.re.kr, jinhyuk@kitech.re.kr, yschoi@kitech.re.kr

Abstract. Cavitation phenomena in a mixed-flow pump are studied using computational fluid dynamics and experiment. Steady-state and transient analyses are conducted using three-dimensional Reynolds-averaged Navier-Stokes equations with a turbulence kinetic energy-specific rate of dissipation (k-ω)-based shear stress transport turbulence model and the homogeneous cavitation model. To observe the pressure fluctuation, five points are monitored during computation. In experiment, a three-axis accelerometer is used for cavitation detection and the vibration characteristics are analyzed. When cavitation occurs, the pressure and vibration magnitudes fluctuate considerably near the blade passing frequency.

1. Introduction

A pump moves fluids through mechanical action. The centrifugal force or thrust created by the rotor blade rotating inside the pump is used to discharge liquid with high pressure. In this process, when the pressure of the fluid is lower than the saturated vapor pressure on the suction side of the impeller, vapor cavities form and begin to grow. These cavities implode and cause shock waves when they reach a high-pressure region, and this cavitation phenomenon causes noise and vibration, reducing the pump performance. Thus, the pump should be operated in a manner that avoids this phenomenon.

To detect cavitation, noise and vibration measurement methods have been used in many studies. For example, Jan et al. [1] measured the cavitation noise and vibration in centrifugal pumps and Ashraf et al. [2] studied cavitation through analysis of acoustic and vibration spectra.

In this paper, the characteristics of a mixed-flow pump under cavitation conditions are studied through numerical analysis and experiment.

2. Target pump

The target mixed-flow pump is one of a series of pumps being developed by the authors [3]. Table 1 lists the specifications of the target pump. The specific speed (N_s), flow coefficient (ϕ), and head coefficient (ψ) are defined as follows:

$$N_s = \frac{\omega\sqrt{Q}}{(gH)^{\frac{3}{4}}} \tag{1}$$

$$\phi = \frac{C_{m2}}{u_2} \tag{2}$$

$$\psi = \frac{2gH}{u_2^2} \tag{3}$$

where ω, Q, g, H, C_{m2}, and u_2 denote the angular velocity, volumetric flow rate, acceleration due to gravity, total head, the meridional component of the absolute velocity at the impeller outlet, and the tangential component of the rotational speed at the impeller outlet, respectively.

Table 1. Target pump specifications.

Item	Value
Specific speed ($Ns_{type\ number}$)	2.43
Flow coefficient (ϕ)	0.19
Head coefficient (ψ)	0.51
Number of blade (impeller)	5
Number of blade (diffuser)	7

3. Numerical Analysis

For the numerical analysis, a computational domain and mesh were generated using ANSYS BladeGen and TurboGrid ver. 18.0, respectively. A hexahedral grid system was employed to generate the mesh and the total domain was composed of 715,905 nodes. The numerical analysis was performed using ANSYS CFX ver. 18.0. To analyze the cavitation phenomena about the target pump, steady and unsteady Reynolds-averaged Navier-Stokes equations were used with a turbulence kinetic energy-specific rate of dissipation (k-ω)-based shear stress transport turbulence model.

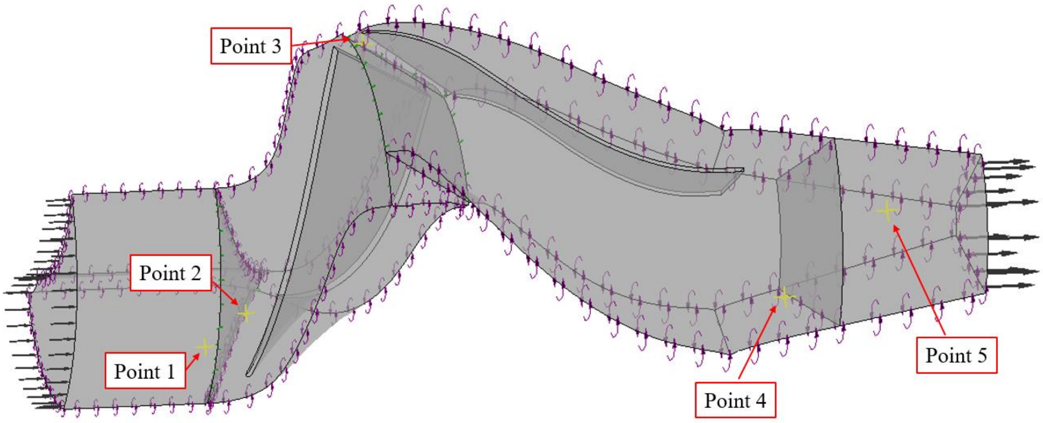

Figure 1. Points for pressure fluctuation monitoring in computational fluid dynamics (CFD).

In the steady state analysis, the interface between the impeller and diffuser was set as-stage averaged. First, to evaluate the non-cavitation condition, the atmospheric pressure and mass flow rate were set at the inlet and outlet, respectively. To determine the net positive suction head required (NPSHr), a computation was performed using a cavitation model derived from the Rayleigh-Plesset equation. The inlet pressure gradually reduced.

In the transient analysis, the interface between the impeller and diffuser was considered in the context of the transient rotor stator method. Seven total impeller rotations were considered, with calculations being performed every 3°. As shown in figure 1, the pressure fluctuations were monitored at five points.

IOP Conf. Series: Earth and Environmental Science **240** (2019) 062032 doi:10.1088/1755-1315/240/6/062032

Points 1 and 2 were located before the impeller, point 3 was located between the impeller and diffuser, and points 4 and 5 were located after the diffuser

4. Experiment

The target pump was tested using an experiment setup consisting of a closed-loop arrangement. This setup satisfied the ISO 5198 standard. To calculate the NPSH, the absolute pressure at the inlet was measured upstream at a point that was twice the inlet flange diameter. The inlet pressure was regulated by the vacuum pump and compressor connected to the tank. The flow rate was measured by a magnetic flowmeter with an accuracy of ±0.2%. While maintaining a constant flow rate, the inlet pressure was changed gradually using a vacuum pump and compressor. The differential pressure between the inlet and outlet was measured to calculate the water head.

A three-axis accelerometer was used to observe the pump vibration characteristics. It was fixed to the bearing cover by magnet. Note that the accelerometer should be located on a solid body, usually on the bearing in the case of a pump, for good accuracy. For real-time fast Fourier transform (FFT) acquisition of the vibration, an IOtech dynamic signal analyzer (DSA; model: 650u) was used. The analysis frequency range was 0 to 1000 Hz and data were obtained in 5-Hz intervals. The vibration value was integrated with the acceleration, because the pump rotation speed was low. Figure 2 shows a schematic view of the test setup and figure 3 shows the location of the accelerometer sensor.

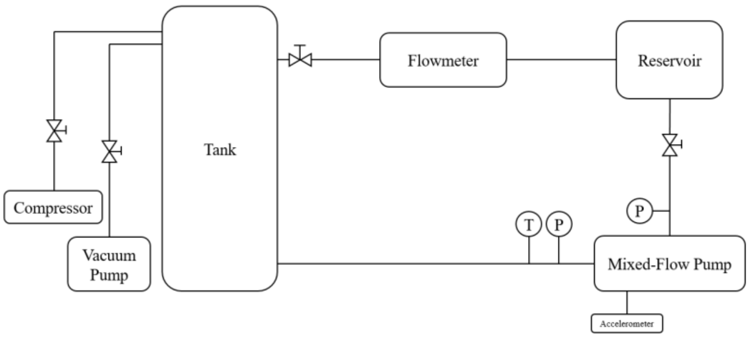

Figure 2. Schematic view of the test setup.

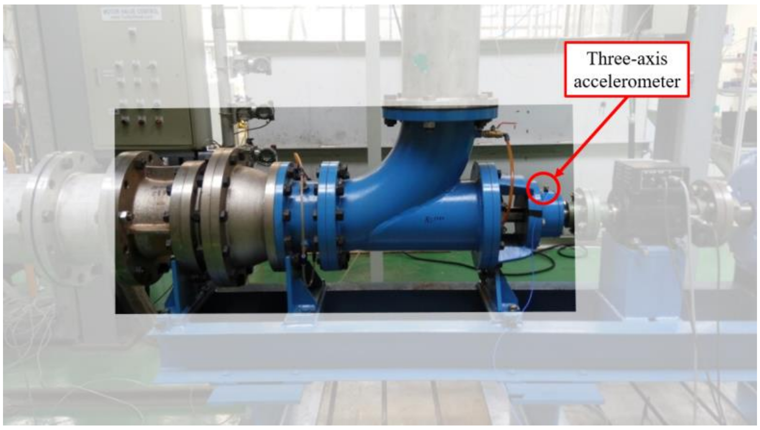

Figure 3. Mixed-flow pump and accelerometer location.

5. Results

Figure 4 shows the variations in the pressure and vibration according to the cavitation coefficient (σ) compared with the total head drop. The *NPSH* and σ are defined as follows:

$$NPSH = \frac{P_{inlet} - P_{vapor}}{\rho g} \tag{4}$$

$$\sigma = \frac{2gNPSH}{u_1^2} \tag{5}$$

where P_{inlet}, P_{vapor}, ρ and u_1 represent the inlet pressure, vapor pressure, the density and the peripheral speed at the impeller inlet, respectively.

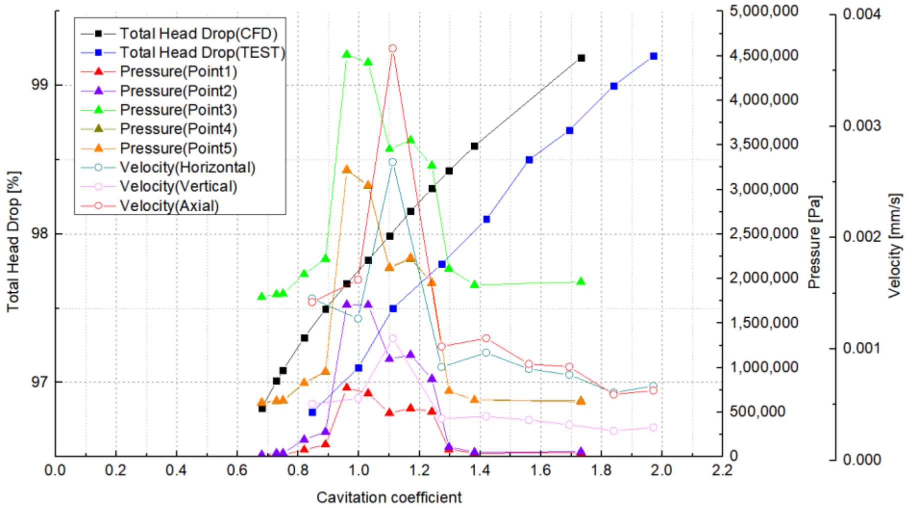

Figure 4. Variation of total head drop, pressure and vibration according to cavitation coefficient.

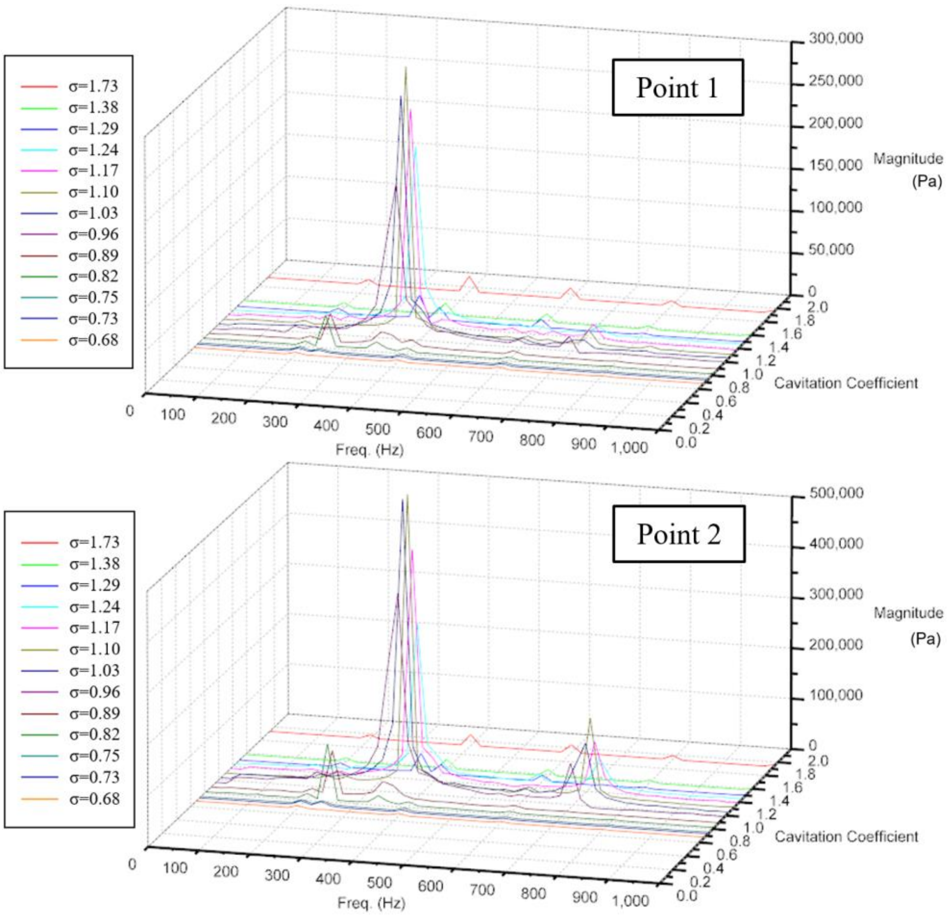

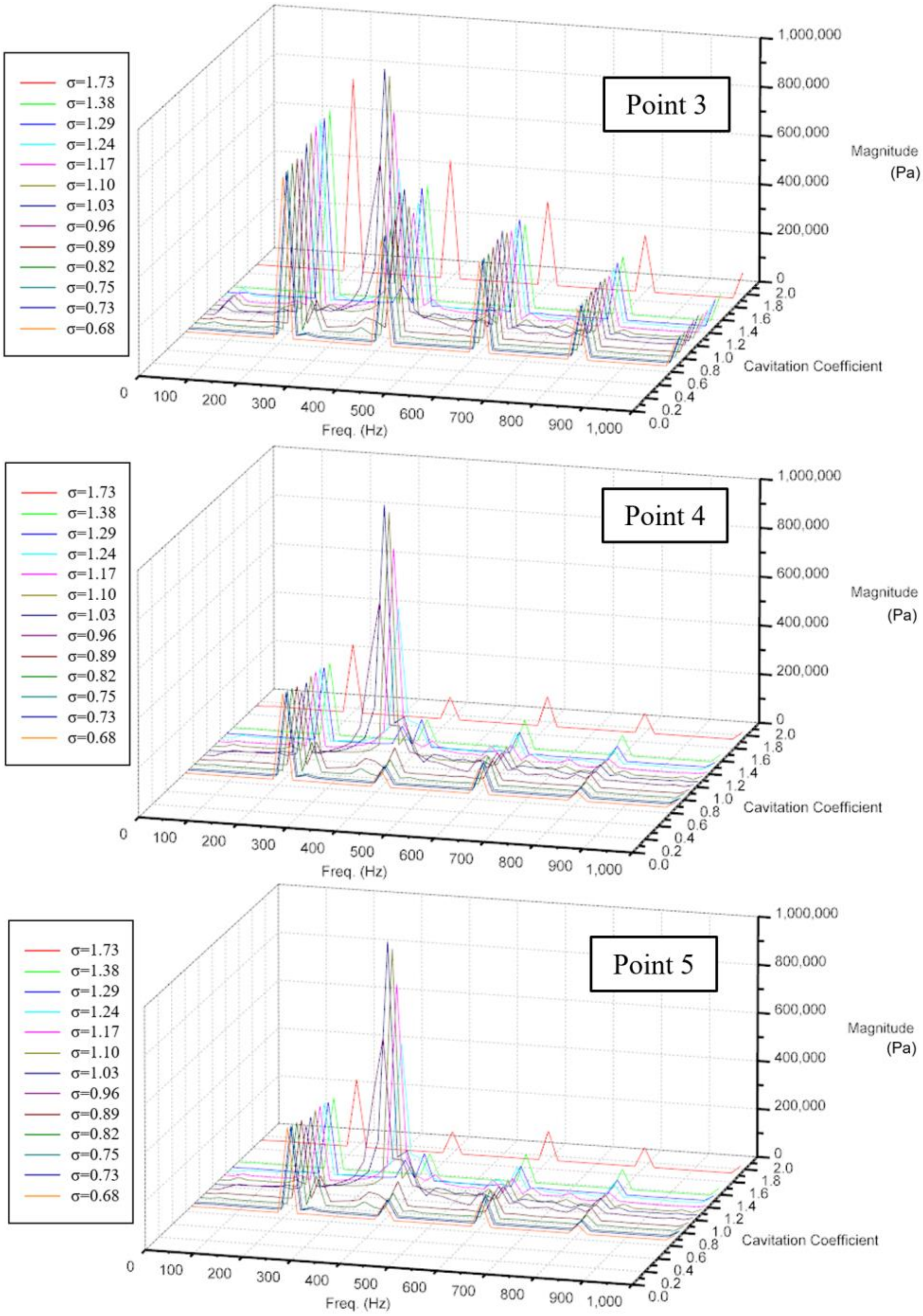

Figure 5. Frequency spectra for pressure distributions from CFD results at design flow rate.

The total head of water decreased as σ decreased. The σ values corresponding to a 3% head drop given by the computational fluid dynamics (CFD) simulation and experimental test were 0.73 and 0.95, respectively. The pressure and vibration magnitudes were calculated by summing all values in the frequency range. As shown in figure 4, as total head decreased, the pressure and vibration magnitudes fluctuated strongly. In particular, when σ was between 0.9 and 1.3, the magnitudes of these properties fluctuated rapidly. For a detailed analysis, FFT was performed; the results are shown in figures 5 and 6.

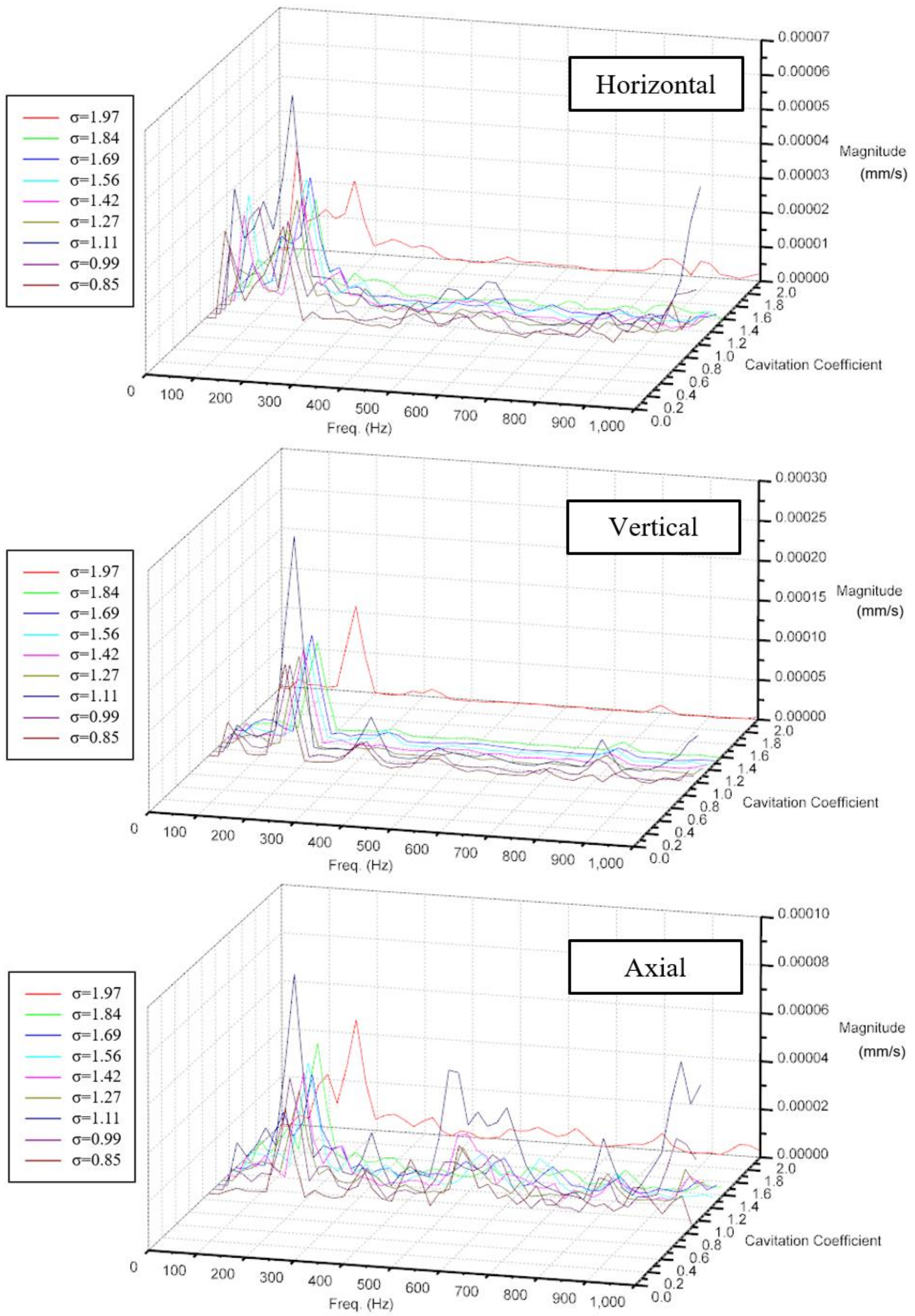

Figure 6. Frequency spectra for vibration distribution in three axis direction at design flow rate.

IOP Conf. Series: Earth and Environmental Science **240** (2019) 062032 doi:10.1088/1755-1315/240/6/062032

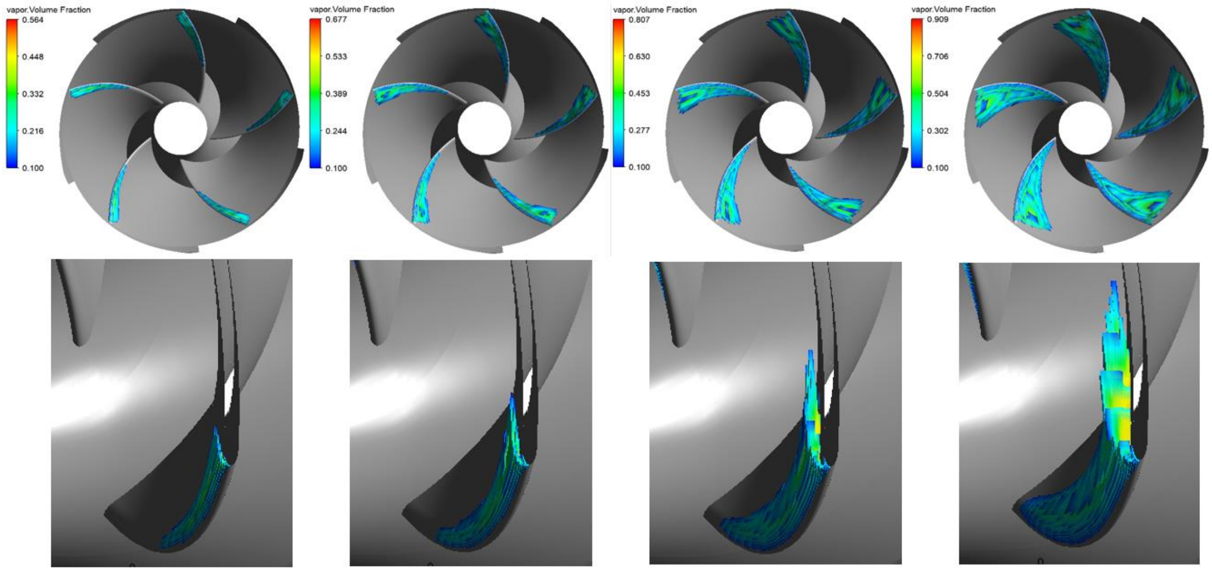

(a) Highest inlet pressure (σ = 1.73)
(b) Initial increase in pressure magnitude (σ = 1.24)
(c) Maximum pressure magnitude (σ = 0.89)
(d) Under the 3% head drop (σ = 0.68)

Figure 7. Distribution of vapor volume fraction.

Figure 5 shows the pressure magnitude distributions in the frequency spectra given by the CFD results at the design flow rate, for the five measurement points. The blade passing frequency (BPF) is clearly apparent in the spectrum obtained at point 3 (between the impeller and diffuser), but is difficult to observe before the impeller (points 1 and 2). This BPF decreased upon passage through the diffuser (points 4 and 5). In each frequency spectrum, the pressure magnitude changed at 260 Hz (near the BPF) and 360 Hz (near the second harmonic of the BPF). These phenomena occurred in all sections of the device and affected the total pressure magnitude. Because no other effects were found in the numerical analysis, this phenomenon can be considered to be caused by cavitation.

The vibration magnitude distributions in the three axial directions are shown in figure 6. A large amount of vibration was clearly observed at the rotation frequency (40 Hz) and the vibration altered near the BPF according to the inlet condition. These vibration changes are less apparent than the pressure fluctuations observed in the CFD results, because many environmental factors such as shaft misalignment and inverter noise affect the data.

Finally, figure 7 shows the distribution of the vapor volume fraction at each inlet condition. Figure 7(b) shows the stage at which the pressure magnitude began to increase rapidly, while figure 7(c) shows the point of maximum pressure magnitude. Vapor occurred on the suction side of the leading edge and expanded continuously into the shroud. When the impeller rotated, the pressure at the suction side of the leading edge dropped under the saturation pressure and, at that moment, a cavity was generated. Because the shroud rotation speed was faster than that of the hub, the cavity occurred closer to the shroud. When the generated cavity reached a high-pressure region, which was from the pressure side of the impeller, the cavity condensed into the water. The distribution expanded as σ decreased. Note that these phenomena cause performance degradation.

6. Conclusion

The pressure and vibration characteristics of a mixed-flow pump were studied. When the cavitation coefficient was between 0.9 and 1.3, and as the inlet pressure decreased, the magnitudes of the pressure and vibrations fluctuated rapidly. These phenomena are known to induce cavitation bubbles. Further, during pressure drops in the pump inlet, noise is absorbed into the two-phase fluid [4]. Moreover, in the frequency spectrum, pressure and vibrations caused by cavitation appeared near the BPF. The magnitudes of this pressure and these vibrations affected the total magnitudes of these properties. In addition, the cavities were observed in the context of the vapor volume fraction distribution. Hence, it was found that cavities occurred at the suction side of the leading edge in particular, near the shroud. These cavities had larger distributions as the cavitation coefficient decreased.

This findings of this study indicate that pressure or vibration measurements can predict the conditions prior to the occurrence of cavitation; therefore, such measurements can be used to prevent this phenomenon and, hence, impede cavitation-induced impeller erosion.

Acknowledgments

This research was supported by a grant (No. 10044860) from the Korea Institute of Industrial Technology Evaluation and Planning (ITEP) that is funded by the Ministry of Science, ICT and Future Planning.

References

[1] J. Cernetic 2009 The use of noise and vibration signals for detection of cavitation in kinetic pumps *Proceedings of the Institution of Mechanical Engineers, Part C: Journal of Mechanical Engineering Science* **223** 1645–55

[2] A. Kotb and A. M. Abdulaziz 2015 Cavitation detection in variable speed pump by analyzing the acoustic and vibration spectrums *Engineering* **7** 706-716

[3] S. Kim, K. Y. Lee, J. H. Kim and Y. S. Choi 2014 A numerical study on the improvement of suction performance and hydraulic efficiency for a mixed-flow pump impeller *Mathnatical Problems in Engineering* **2014** Article ID 269483

[4] D. H. Lee and S. C. Kang 2013 Prognostic technique for pump cavitation erosion *The Korean Society of Mechanical Engineers* **37** 1021–27

[5] M. Chudina 2003 Noise as an indicator of cavitation in a centrifugal pump *Acoustical Physics* **49** 463-74

[6] N. Zhang, M. Yang, B. Gao and Z. Li 2015 Vibration characteristics induced by cavitation in a centrifugal pmp with slope volute *Shock and Vibration* **2015** article ID 294980

[7] M. Sedlar, O. Sputa and M. Komarek 2012 CFD analysis of cavitation phenomena in mixed-flow pump *International Journal of Fluid Machinery and Systems* **5** 18-29